

separated sufficiently to accommodate the tube itself or a hollow Pyrex water thermostated condenser in which the Guoy tube could be freely suspended.

Measurements were first made on each species at room temperature after flushing the solutions with nitrogen. Density was determined by pycnometer. The field was maintained at 8000 G for these measurements, by using 4-in. pole caps at a separation of 1 in. and a current of 6.2 A.

For the second set of measurements, the water-jacketed cavity was used to maintain constant temperature. The Guoy tube, suspended in the cavity, was allowed to come to equilibrium with its surrounding for about 1 h or until readings with the field off were constant. The temperature of the cavity, assumed to be the same as the temperature of the sample, was determined by hanging a NBS mercury thermometer in the cavity, under the same conditions. The pole gap was increased to 2 in. to accommodate the water jacket, and the field was

reduced to 6000 G at the same amperage (6.2 A). The temperature range covered was limited because of the decomposition of the dimers at high temperatures.

**Acknowledgment.** The authors wish to express their indebtedness to Professor J. W. Wrathall for the use of the Guoy apparatus and to Dr. J. B. Spencer for making the electron spin resonance measurements. The original research was supported by the Atomic Energy Commission and present research is supported by the Division of Chemical Sciences, Office of Basic Energy Sciences, United States Department of Energy, under Contract No. W-7405-ENG-48.

**Registry No.** SBD, 77153-84-5; DBD, 23852-05-3;  $[\text{Cr}(\text{H}_2\text{O})_6]^{3+}$ , 14873-01-9;  $[(\text{H}_2\text{O})_4\text{Cr}(\text{OH})_2\text{Cr}(\text{H}_2\text{O})_2(\text{OH})_2\text{Cr}(\text{H}_2\text{O})_4]^{5+}$ , 60938-70-7.

Contribution from the Department of Chemistry,  
Clarkson College of Technology, Potsdam, New York 13676

## Normal-Coordinate Analyses for the Vibrations of Tetraphenyl- and Tetramethyldithioimidodiphosphate and the Adamantane-like Cage Structure $\text{Cu}_4\text{S}_6$

O. SIIMAN

Received September 22, 1980

Normal-coordinate analyses have been performed for 1:1 metal-ligand models of bis(tetraphenyldithioimidodiphosphinato)manganese(II) and bis(tetramethyldithioimidodiphosphinato)cobalt(II) and for the  $\text{Cu}_4\text{S}_6$  core of the tris(tetraphenyldithioimidodiphosphinato)tetracopper(I) cation in  $C_2$  and  $T_d$  point symmetries, respectively. Results of the calculations support the assignment of  $\nu_{\text{as}}(\text{PNP})$  and  $\nu_s(\text{PNP})$  to bands near 1210 and 820  $\text{cm}^{-1}$ ,  $\nu(\text{PC})$  to bands between 680 and 750  $\text{cm}^{-1}$ ,  $\nu_{\text{as}}(\text{PS})$  and  $\nu_s(\text{PS})$  to bands between 500 and 600  $\text{cm}^{-1}$ , and  $\nu_{\text{as}}(\text{MS})$  and  $\nu_s(\text{MS})$  to bands between 240 and 320  $\text{cm}^{-1}$ . Bonding stretching force constants show that Co-S bonds in the tetramethyl compound are stronger than Mn-S bonds in the tetraphenyl compound, and this is compensated by a lower  $K(\text{P-S})$  value in the Co(II) complex. The lack of infrared and Raman intensity in  $\nu_s(\text{PNP})$  is explained in terms of opposing  $\sigma$  and  $\pi$  contributions to the dipole moment and polarizability changes during the symmetric PNP stretching vibration. Only in resonance Raman spectra where other contributions to the band intensity are operative was  $\nu_s(\text{PNP})$  observed. Analysis of the  $\text{Cu}_4\text{S}_6$  cluster vibrations showed that only weak Cu...Cu bonding interactions were present.  $\nu(\text{Cu(I)-S})$  modes were located between 280 and 170  $\text{cm}^{-1}$  in the infrared and Raman spectra. The  $K(\text{Cu-S})$  value was about the same magnitude as  $K(\text{Mn-S})$  for the bis chelate.

### Introduction

Dithioimidodiphosphinates,  $\text{SPR}_2\text{NR}_2\text{PS}^-$ , where R = phenyl (L) or methyl (L'), coordinate to divalent first-row transition-metal ions to form bis complexes<sup>1</sup> that contain a tetrahedral  $\text{M}^{\text{II}}\text{S}_4$  core geometry. The preference for tetrahedral<sup>2,1b</sup> over square-planar geometry, even for the nickel complex, was thought at first to reflect a low ligand field strength with this bidentate sulfur ligand. Yet analyses of ligand field spectra<sup>1a,b</sup> of Mn(II), Fe(II), Co(II), and Ni(II) complexes showed that  $\text{L}^-$  presented a field of intermediate strength. To clarify the metal-sulfur and chelate ring bonding picture in these chelates, we undertook an infrared-Raman spectral study<sup>1d</sup> and herein present the results of normal-coordinate calculations on several metal dithioimidodiphosphinates.

Measurement of Raman intensities has been useful in studies of molecular structure and bonding, particularly in the estimation of bond orders. In the theory of Raman intensities the mean molecular polarizability,  $\bar{\alpha}$ , is directly related<sup>3</sup> to the observed intensity of a totally symmetric Raman band. Approximate methods have been devised<sup>4</sup> to express terms in the

molecular polarizability derivative as a superposition of principal polarizability components of individual bonds. Bond polarizabilities,  $\bar{\alpha}_u$ , are related to molecular polarizabilities by the equation

$$\frac{\partial \bar{\alpha}}{\partial Q_i} = \sum_u l_{ui} \frac{\partial \bar{\alpha}_u}{\partial R_u}$$

where  $l_{ui}$  is the L matrix (eigenvectors for the normal vibrations  $Q_i$ ) element between internal coordinates  $R_u$  and  $Q_i$ . The sum is taken over bonds,  $u$ . We suggest that further division of bond polarizabilities into two components,  $\sigma$  and  $\pi$ , may be justified in cases where the two contributions occur in opposing directions, i.e., are of opposite sign. One of the apparent anomalies in the vibrational spectra of imidodiphosphinates<sup>1d,5</sup> was the absence of any intensity in the symmetric  $\text{P}=\text{N}=\text{P}$  stretching band in either infrared or Raman spectra. Only in resonance Raman spectra was it observed. The reasons for a very small change in polarizability as well as in dipole moment with respect to this normal coordinate are explored in terms of  $\sigma$  and  $\pi$  bonding in the imidodiphosphinate group.

Short Cu...Cu distances within several copper cluster compounds have been cited as evidence for some metal-metal bonding.<sup>6</sup> Raman intensities of metal cluster<sup>7</sup> related vibrational bands are expected to depend on the extent of metal-metal interaction. Since Cu...Cu distances in the

- (1) (a) Davison, A.; Switkes, E. S. *Inorg. Chem.* **1971**, *10*, 837. (b) Siiman, O.; Gray, H. B. *Ibid.* **1974**, *13*, 1185. (c) Bereman, R. D.; Wang, F. T.; Najdzionek, J.; Braitsch, D. M. *J. Am. Chem. Soc.* **1976**, *98*, 7266. (d) Siiman, O.; Vetuskey, J. *Inorg. Chem.* **1980**, *19*, 1672.
- (2) (a) Churchill, M. P.; Cooke, J.; Fennessey, J. P.; Wormald, J. *Inorg. Chem.* **1971**, *10*, 1031. (b) Churchill, M. P.; Wormald, J. *Ibid.* **1971**, *10*, 1778.
- (3) Hester, R. E. In "Raman Spectroscopy, Theory and Practice"; Szymanski, H. A., Ed.; Plenum Press: New York, 1967; Chapter 4.
- (4) Long, D. A. *Proc. R. Soc. London, Ser. A* **1953**, *217*, 203.

- (5) Siiman, O.; Huber, C. P.; Post, M. L. *Inorg. Chim. Acta* **1977**, *25*, L11.
- (6) Fackler, J. P., Jr. *Prog. Inorg. Chem.* **1976**, *21*, 55.
- (7) (a) Quicksall, C. O.; Spiro, T. G. *Inorg. Chem.* **1970**, *9*, 1045. (b) Maroni, V. A.; Spiro, T. G. *Ibid.* **1968**, *7*, 193.

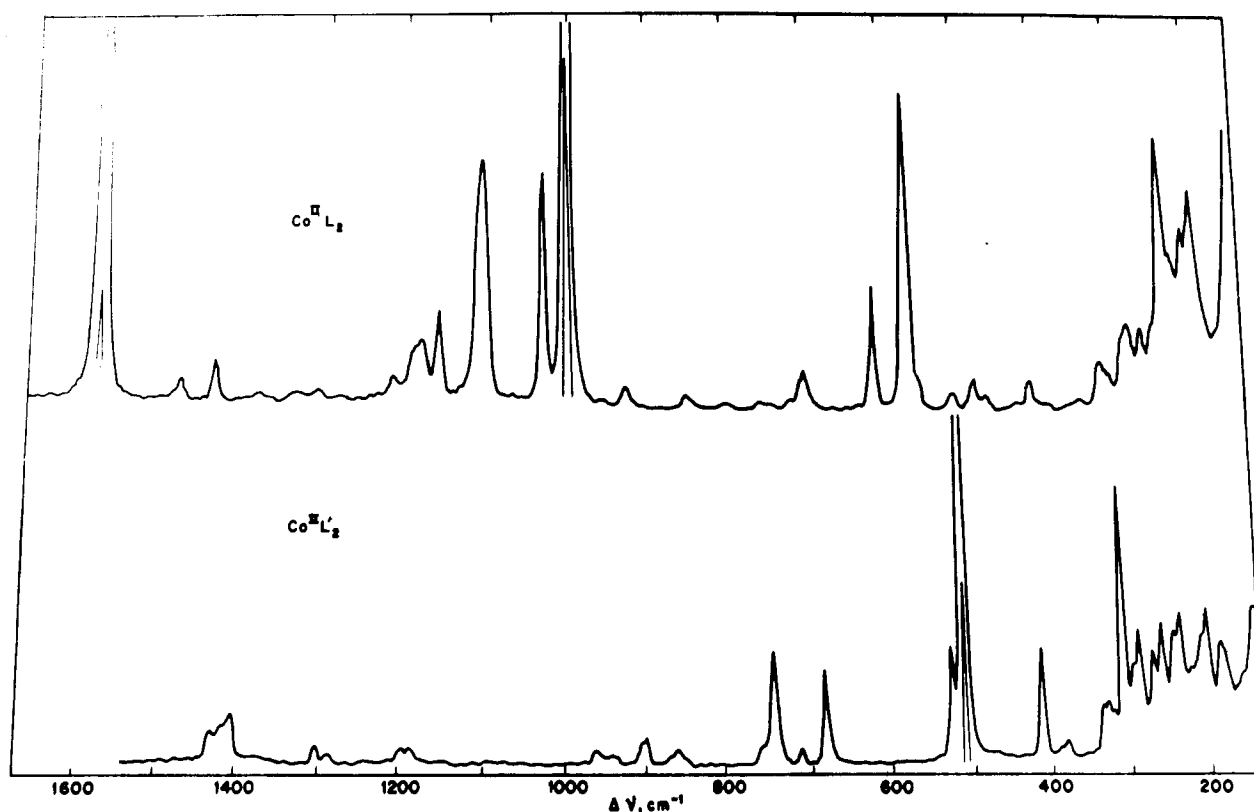


**Figure 1.** Raman spectra of solid samples. Experimental conditions [excitation (nm), power (mW), slit width ( $\text{cm}^{-1}$ ), sensitivity (counts/s), time constant (s), scan rate ( $\text{cm}^{-1}/\text{s}$ )]: for  $\text{Co}^{\text{II}}\text{L}_2$ , 488.0 ( $\text{Ar}^+$ ), 20, 9.8, 2000, 1, 1; for  $\text{Co}^{\text{II}}\text{L}'_2$ , 488.0 ( $\text{Ar}^+$ ), 200, 4.8, 4000, 2, 0.5.

**Table I.** Chelate Ring and P-C Stretching-Mode Frequencies ( $\text{cm}^{-1}$ )

	$\text{Mn}^{\text{II}}\text{L}_2$		$\text{Co}^{\text{II}}\text{L}_2$		$\text{Co}^{\text{II}}\text{L}'_2$		$\text{Cu}^{\text{I}}_4\text{L}_3^+$	
	IR	R	IR	R	IR	R	IR	R
$\nu_{\text{as}}(\text{PN})$	1218 vs	...	1215 vs	1215 w	1198 vs	1198 vw	1216 vs	...
$\nu(\text{PC})$	715 m	718 vw	715 m	718 vw	1187 vs	1187 vw	718 m	...
	700 vs	705 mw	700 vs	704 mw	749 m	749 m	...	700 vw
	692 sh	...	692 sh	...	713 m	718 vw	...	...
$\nu_{\text{as}}(\text{PS})$	568 vs	567 w, sh	565 vs	560 sh	674 vs	684 m	692 vs	...
$\nu_{\text{s}}(\text{PS})$	585 mw	580 s	...	572 s	505 m	...	551 vs	...
$\nu_{\text{s}}(\text{MS})$	...	245 s	...	240 s	...	306 ms	570 vs, sh	570 s
$\nu_{\text{as}}(\text{MS})$	275 w	275 w	...	270 mw	...	...	575 s	272 vs
	285 w	285 w	...	288 mw	318 m	...	242 m	245 w

tetraphenyldithioimidodiphosphinate-Cu(I) cluster,<sup>8</sup>  $\text{Cu}^{\text{I}}_4\text{L}_3^+$ , were smaller than the sum of van der Waals radii but larger than the sum of covalent radii, the influence of metal-metal bonding on intensities of  $\nu(\text{Cu-S})$  Raman bands was of interest. Vibrations of the copper-sulfur clusters were further analyzed.

### Experimental Section

The preparation of all compounds was discussed in a previous paper.<sup>1d</sup> Raman spectra were recorded with a Jarrell-Ash 25-500 double Ebert monochromator using a water-cooled Hammamatsu R500 photomultiplier tube for detection. A Spectra-Physics Model 165 argon- or krypton-ion laser was used for excitation. Samples were rotated in a cylindrical stainless-steel cell, which had a circular groove packed with powdered material. Incident laser light reached the sample at an angle of  $\sim 45^\circ$ . Scattered light was collected at  $90^\circ$  to the incident beam.

### Results and Discussion

#### A. Infrared and Raman Spectra. 1. P-C and Chelate Ring Stretching Vibrations.

IR and Raman (R) spectra of  $\text{Mn}^{\text{II}}\text{L}_2$ ,

$[\text{Cu}^{\text{I}}_4\text{L}_3^+][\text{Cu}^{\text{I}}\text{Cl}_2^-]\text{CCl}_4$ , and  $[\text{Cu}^{\text{I}}_4\text{L}_3^+][\text{ClO}_4^-]$  and the IR spectrum of  $\text{Co}^{\text{II}}\text{L}'_2$  were previously<sup>1d</sup> recorded. The IR spectrum of  $\text{Co}^{\text{II}}\text{L}_2$  is very similar to that of  $\text{Mn}^{\text{II}}\text{L}_2$ . R spectra of  $\text{Co}^{\text{II}}\text{L}_2$  and  $\text{Co}^{\text{II}}\text{L}'_2$  between 1600 and  $100\text{ cm}^{-1}$  are shown in Figure 1. Electronic absorption spectra of the Co(II) complexes indicated<sup>1a</sup> that they too contain a tetrahedral  $\text{Co}^{\text{II}}\text{S}_4$  core that was verified by single-crystal X-ray analyses<sup>1b,2</sup> for  $\text{Mn}^{\text{II}}\text{L}_2$  and for  $\text{Fe}^{\text{II}}\text{L}'_2$  and  $\text{Ni}^{\text{II}}\text{L}'_2$ . Vibrational assignments for phosphorus-neighboring atom, phenyl ring, and some metal-sulfur IR and R bands were made before.<sup>1d</sup> With a few revisions the chelate ring and  $\nu(\text{P-C})$  band assignments are summarized in Table I. In all compounds chelated L and L' showed a broad intense  $\nu_{\text{as}}(\text{PNP})$  infrared band near  $1200\text{ cm}^{-1}$  and a very weak Raman counterpart. One very intense  $\nu(\text{P-C})$  infrared band occurs at or below  $700\text{ cm}^{-1}$ . Weak  $\nu(\text{P-C})$  Raman bands were observed when R = phenyl whereas medium R bands occur at  $749$  and  $684\text{ cm}^{-1}$  when R = methyl. The tetraphenyl derivatives show a lower frequency strong  $\nu_{\text{as}}(\text{P-S})$  IR band and a higher frequency strong R band,  $\nu_{\text{s}}(\text{P-S})$ . With the acquisition of the R spectrum of  $\text{Co}^{\text{II}}\text{L}'_2$  our revised assignments of L' chelates show a similar trend but a smaller frequency difference between  $\nu_{\text{as}}(\text{P-S})$  at  $506$

(8) Huber, C. P.; Post, M. L.; Siiman, O. *Acta Crystallogr., Sect. B* 1978, B34, 2629.

$\text{cm}^{-1}$ , an intense IR band, and  $\nu_s(\text{P}\cdots\text{S})$  at  $511\text{ cm}^{-1}$ , an intense R band. The strongest low-frequency Raman band is observed near  $240\text{ cm}^{-1}$  in  $\text{Mn}^{\text{II}}\text{L}_2$  and  $\text{Co}^{\text{II}}\text{L}_2$  but at  $306\text{ cm}^{-1}$  in  $\text{Co}^{\text{II}}\text{L}'_2$ . In L chelates, it was previously assigned<sup>1d</sup> to  $\nu_s(\text{M}-\text{S})$  on the basis of vibrational fine structure in the low-temperature single-crystal electronic absorption spectrum<sup>1b</sup> of  $\text{Mn}^{\text{II}}\text{L}_2$ . In the comparison of methyl against phenyl derivative chelate stretching frequencies, the methyl shows a higher  $\nu_s(\text{Co}-\text{S})$ ,  $\Delta = 66\text{ cm}^{-1}$ , but a lower  $\nu(\text{P}\cdots\text{S})$ ,  $\Delta = 45$  or  $60\text{ cm}^{-1}$ , and  $\nu_{\text{as}}(\text{P}\cdots\text{N}\cdots\text{P})$ ,  $\Delta = 23\text{ cm}^{-1}$ . Very nearly the same lowering of  $\nu(\text{P}=\text{S})$  and  $\nu_{\text{as}}(\text{P}-\text{N}-\text{P})$  frequencies was observed in comparing the respective ligand, HL and HL', band frequencies:  $\nu(\text{P}=\text{S})$ ,  $\Delta = 52$  or  $64\text{ cm}^{-1}$ ;  $\nu_{\text{as}}(\text{P}-\text{N}-\text{P})$ ,  $\Delta = 18\text{ cm}^{-1}$ . In addition,  $\nu(\text{PS})$  band positions of HL (HL') compared to chelated L (L') were  $\sim 60\text{ cm}^{-1}$  lower in  $\text{Co}^{\text{II}}\text{L}_2$  ( $\text{Co}^{\text{II}}\text{L}'_2$ ). Therefore, the higher  $\nu_s(\text{Co}-\text{S})$  frequency in  $\text{Co}^{\text{II}}\text{L}'_2$  might not directly be linked to the further lowering of ligand  $\nu(\text{PS})$  and  $\nu(\text{PNP})$  band frequencies. A change in coupling of other lower frequency modes to  $\nu(\text{M}-\text{S})$  may be involved. Force constants derived from normal-coordinate calculations offer a more reliable basis for comparing metal-sulfur bond strengths.

**2. Chelate Ring Bending Modes.** Analysis of the distribution of vibrations in the  $C_2$  symmetry 10-atom model of  $\text{MS}_2\text{P}_2\text{R}_4\text{N}$  shows that the 12 A + 12 B normal vibrations can be divided into 5 bond stretching modes, 3 ring angle bending modes, and 4 P-R bending modes for each representation. The five stretching modes,  $\nu(\text{PN})$ ,  $\nu(\text{PS})$ ,  $\nu(\text{MS})$ , and two  $\nu(\text{PR})$ , were previously<sup>1d</sup> identified. One ring bending mode from the A and the B species predominantly involves  $\delta(\text{PNP})$  and  $\delta(\text{SPN})$ , respectively. These are expected to be the highest frequency ring bending vibrations.  $\delta(\text{PNP})$  belongs to A species normal modes and is both IR and R active in  $C_2$  symmetry. The Raman band is expected to be more intense than its IR counterpart. Phosphonitrilic trimers exhibit<sup>9</sup> the following  $\text{P}_3\text{N}_3$  ring bending vibrations: in-plane ring deformations at  $669\text{ cm}^{-1}$  ( $a'_1$ ) and  $529\text{ cm}^{-1}$  ( $e'$ ); out-of-plane ring deformations at  $619\text{ cm}^{-1}$  ( $a''_2$ ) and  $202\text{ cm}^{-1}$  ( $e''$ ). Since some of the ring stretching modes,  $\nu_s(\text{PNP})$  and  $\nu_s(\text{PS})$ , appeared very intense in the resonance Raman (RR) spectrum of  $\text{Cu}^{\text{II}}\text{L}_2$ , we expect that bands due to symmetric bending modes that are associated with SPNPS in the chelate ring might be enhanced to a similar degree. This is especially appropriate since extensive mixing of the totally symmetric  $\nu(\text{PNP})$  and  $\delta(\text{PNP})$  modes was proposed in one Raman study<sup>9b</sup> of phosphonitrilic trimers. An intense RR band at  $420\text{ cm}^{-1}$  in  $\text{Cu}^{\text{II}}\text{L}_2$  is therefore assigned to  $\delta_s(\text{PNP})$  with some mixing with  $\nu_s(\text{PNP})$ . Medium-intensity normal-Raman bands at  $420\text{ cm}^{-1}$  in  $\text{Mn}^{\text{II}}\text{L}_2$  and other L chelates and at  $410\text{ cm}^{-1}$  in  $\text{Co}^{\text{II}}\text{L}'_2$  are also assigned to  $\delta_s(\text{PNP})$ . The slightly lower  $\delta_s(\text{PNP})$  frequency in  $\text{Co}^{\text{II}}\text{L}'_2$  parallels a lower  $\nu_{\text{as}}(\text{PNP})$  frequency in the IR spectrum of  $\text{Co}^{\text{II}}\text{L}'_2$  relative to  $\text{Co}^{\text{II}}\text{L}_2$ . IR and R spectra<sup>10</sup> of the centrosymmetric compound bis(dimethylphosphine) disulfide show that it has no other IR or R bands between  $550$  and  $300\text{ cm}^{-1}$  apart from an intense R band at  $437\text{ cm}^{-1}$  for  $\nu(\text{P}-\text{P})$ . Another RR band in  $\text{Cu}^{\text{II}}\text{L}_2$  appears weakly at  $530\text{ cm}^{-1}$ . Since the remaining RR bands at  $213$  and  $287\text{ cm}^{-1}$  in  $\text{Cu}^{\text{II}}\text{L}_2$  can be assigned to symmetric and asymmetric  $\nu(\text{Cu}-\text{S})$  modes, we tentatively assign the  $530\text{ cm}^{-1}$  band to the highest frequency asymmetric B species ring deformation. Spectra of  $\text{M}^{\text{II}}\text{L}_2$  complexes show a medium IR and a weak R band in this region. A medium-weak IR and R band at  $524\text{ cm}^{-1}$  in  $\text{Co}^{\text{II}}\text{L}'_2$  is also observed. Other ring-deformation modes are expected at lower frequencies since they are metal dependent

Table II<sup>a</sup>

	$\delta_s(\text{CH}_3)$	$\delta_{\text{as}}(\text{CH}_3)$	$\rho_r(\text{CH}_3)$	$\text{CH}_3$ wag
IR	1299 s	1422 w	965 w	863 s
	1288, 1285 s	1411 ms	943 s	853 w
		1397 w	932 s	
			896 ms	
R	1300 w	1426 w	962 w	860 w
	1288 vw	1418 vw	942 vw	
		1403 w	935 vw	
			900 w	

<sup>a</sup> Units:  $\text{cm}^{-1}$ .

or have a torsional mode contribution.

Raman spectra of both HL and HL' ligands show medium bands near  $408$  and  $388\text{ cm}^{-1}$ , respectively, which occur very weakly in the IR spectra and are  $\sim 20\text{ cm}^{-1}$  downshifted from Raman bands that were assigned to  $\delta(\text{PNP})$  in the metal chelates. Although bond stretching modes,  $\nu(\text{P}\cdots\text{N}\cdots\text{P})$  in metal complexes and  $\nu(\text{P}-\text{N}-\text{P})$  in protonated ligands, differ widely in frequency due to the change in bonding, we do not expect very much difference in the bending mode,  $\delta(\text{P}\cdots\text{N}\cdots\text{P})$  and  $\delta(\text{P}-\text{N}-\text{P})$ , frequencies. Therefore,  $\delta(\text{PNP})$  in the ligands is assigned to bands at  $408$  and  $388\text{ cm}^{-1}$ .

**3.  $\text{PR}_2$  and  $\text{CH}_3$  Group Bending Vibrations.**  $\delta(\text{P}-\text{CH}_3)$  bands in bis(tetramethylphosphine) disulfide are observed<sup>10</sup> between  $300$  and  $150\text{ cm}^{-1}$ . Four bands, as in tetramethyl-dithioimidodiphosphinates, are predicted and are observed in the R spectrum of the solid at  $290$  (s),  $230$  (mw),  $208$  (mw), and  $177$  (s)  $\text{cm}^{-1}$ . Four similar bands occur in the R spectrum of  $\text{Co}^{\text{II}}\text{L}'_2$  as doublets with the more intense peaks of the pairs at  $286$ ,  $234$ ,  $198$ , and  $181\text{ cm}^{-1}$ . An extra R band is found at  $257\text{ cm}^{-1}$ . Geometric nonequivalence of the two ligands in  $\text{Co}^{\text{II}}\text{L}'_2$  might explain the presence of doublet R bands associated with  $\delta(\text{P}-\text{CH}_3)$ . Similar splitting of methyl group vibrational bands (vide infra) is observed in the IR and R spectra of  $\text{Co}^{\text{II}}\text{L}'_2$ . The  $\text{P}-\text{CH}_3$  bending modes are distributed into four basic types of motion that occur, in general, for  $\text{XY}_2$  groups:  $\text{PMe}_2$  deformation (scissor), twist, rock, and wag. Analysis of characteristic methyl group vibrations shows that two symmetrical deformations, four asymmetrical deformations, four rocking modes, and two wagging modes are assignable to both A and B species as shown in Table II.  $\delta$ -(P-Ph) modes should be located at lower frequency from corresponding  $\delta(\text{P}-\text{CH}_3)$  ones. Three medium-to-strong R bands that fit this description are found between  $150$  and  $300\text{ cm}^{-1}$  in both HL and HL' ligands:  $258$ ,  $223$ , and  $164\text{ cm}^{-1}$  in HL;  $285$ ,  $225$ , and  $182\text{ cm}^{-1}$  in HL'. Some of the bands in  $\text{Co}^{\text{II}}\text{L}_2$  at  $290$ ,  $270$ ,  $240$ ,  $212$ , and  $200\text{ cm}^{-1}$  may, thus, be assigned to  $\delta(\text{P}-\text{Ph})$  vibrations.

**B. Normal-Coordinate Analyses. 1.  $\text{MnL}_2$  and  $\text{CoL}_2$ .** Since the chelate rings of  $\text{Mn}^{\text{II}}\text{L}_2$  were found by X-ray analysis<sup>1b</sup> to have very nearly an  $S_4$  axis of symmetry down the N-Mn-N line, a 1:1 metal-ligand model possessing  $C_2$  symmetry, shown in Figure 2, was adopted for normal-mode calculations. The phenyl group carbon and hydrogen atoms were treated as a single mass to simplify the calculations. Previous calculations<sup>11</sup> have shown this approximation to be justified, but it does lead to an overestimation of some force constants associated with the R group. Geometric parameters that were used are shown in Table III.

The 24 normal vibrations possible after excluding translations and rotations (12 A + 12 B) were analyzed. The 10-atom model gave 32 internal (10 bond stretching, 16 angle bending, and 6 torsional angle bending) coordinates, which could be

(9) (a) Chapman, A. C.; Paddock, N. L. *J. Chem. Soc.* **1962**, 635. (b) Adams, D. M.; Fernando, W. S. *J. Chem. Soc., Dalton Trans.* **1972**, 2503. (c) Creighton, J. A.; Thomas, K. M. *Spectrochim. Acta, Part A* **1973**, *29A*, 1077.

(10) (a) Cowley, A. H.; Steinfink, H. *Inorg. Chem.* **1965**, *4*, 1827. (b) Siiman, O., unpublished results.

(11) Siiman, O.; Fresco, J. *Inorg. Chem.* **1971**, *10*, 297.

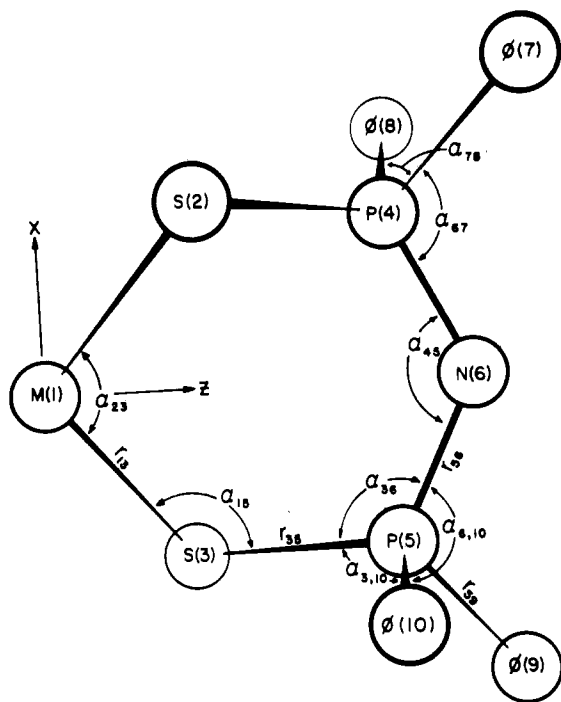
Figure 2. The 1:1 metal-ligand model for  $ML_2$ .

Table III. Geometric Parameters for Metal-Ligand Models

	av values			idealized values for $C_2$ symmetry		av values for $T_d Cu_4 S_6$
	$Mn^{II}L_2$	$Fe^{II}L'$	$Ni^{II}L'$	$Mn^{II}L_2$	$Co^{II}L'$	
$r_{M-S}$ , Å	2.443	2.360	2.282	2.443	2.321	2.266 <sup>a</sup>
$r_{P-S}$ , Å	2.013	2.020	2.023	2.013	2.022	2.053
$r_{P-N}$ , Å	1.588	1.591	1.580	1.588	1.586	1.579
$r_{P-Ph}$ , Å	1.815	1.806	1.825	1.815	1.816	1.799
$\alpha_{SMS}$ , deg	111.9	109.3	109.5	111.6	111.0	123.6
$\alpha_{MSP}$ , deg	99.9	99.5	104.6	99.9	102.1	102.5
$\alpha_{SPN}$ , deg	118.7	116.7	116.6	118.2	116.6	118.2
$\alpha_{PNP}$ , deg	133.5	132.3	128.4	133.5	130.4	138.0
$\alpha_{SPPH}$ , deg	107.9	107.9	107.6	107.9	108.3	106.7
$\alpha_{NPPH}$ , deg	107.8	109.0	108.6	107.9	108.3	108.8
$\alpha_{PhPPH}$ , deg	106.1	105.7	107.2	106.3	106.5	107.2

<sup>a</sup> Idealized value for  $T_d Cu_4 S_6$  symmetry 2.263 Å.

divided into the 17 A and 15 B symmetry coordinates listed in Table IV. Torsional ring angle bending coordinates were introduced after it was discovered that a complete set of 12 A + 12 B nonzero frequencies was not obtained with the listed stretching and bending coordinates alone. The redundancies, 5 A + 3 B, yielded zero frequencies in the eigenvalue problem. Diagonalization of the G matrices for A and B also gave 5 A + 3 B zero eigenvalues, demonstrating the presence of this number of dependent coordinates in the symmetry coordinate sets. The GF matrix problem was solved by procedures similar to the ones described previously.<sup>12</sup> Modified Urey-Bradley

Table IV. Symmetry Coordinates for 1:1 Metal-Ligand Model of Bis(tetraphenyldithioimidodiphosphinato)manganese(II) in  $C_2$  Symmetry

coordinate	mode
A Species	
$S_1 = (1/2^{1/2})(\Delta r_{46} + \Delta r_{56})$	$\nu(P\cdots N)$
$S_2 = (1/2^{1/2})(\Delta r_{47} + \Delta r_{59})$	$\nu(P-Ph)$
$S_3 = (1/2^{1/2})(\Delta r_{48} + \Delta r_{5,10})$	$\nu(P-Ph)$
$S_4 = (1/2^{1/2})(\Delta r_{24} + \Delta r_{35})$	$\nu(P\cdots S)$
$S_5 = (1/2^{1/2})(\Delta r_{12} + \Delta r_{13})$	$\nu(Mn-S)$
$S_6 = (1/2)(\Delta\alpha_{67} + \Delta\alpha_{68} + \Delta\alpha_{69} + \Delta\alpha_{6,10})$	$\delta(NPPH)$
$S_7 = (1/2)(\Delta\alpha_{67} - \Delta\alpha_{68} + \Delta\alpha_{69} - \Delta\alpha_{6,10})$	$\delta(NPPH)$
$S_8 = (1/2)(\Delta\alpha_{27} + \Delta\alpha_{28} + \Delta\alpha_{39} + \Delta\alpha_{3,10})$	$\delta(SPPH)$
$S_9 = (1/2)(\Delta\alpha_{27} - \Delta\alpha_{28} + \Delta\alpha_{39} - \Delta\alpha_{3,10})$	$\delta(SPPH)$
$S_{10} = (1/2^{1/2})(\Delta\alpha_{78} + \Delta\alpha_{9,10})$	$\delta(PhPPH)$
$S_{11} = \Delta\alpha_{45}$	$\delta(PNP)$
$S_{12} = (1/2^{1/2})(\Delta\alpha_{26} + \Delta\alpha_{36})$	$\delta(SPN)$
$S_{13} = (1/2^{1/2})(\Delta\alpha_{14} + \Delta\alpha_{15})$	$\delta(MnSP)$
$S_{14} = \Delta\alpha_{33}$	$\delta(SMnS)$
$S_{15} = (1/2^{1/2})(\Delta\tau_{1246} + \Delta\tau_{1356})$	$\tau(MnSPN)$
$S_{16} = (1/2^{1/2})(\Delta\tau_{2465} + \Delta\tau_{3564})$	$\tau(SPNP)$
$S_{17} = (1/2^{1/2})(\Delta\tau_{3124} + \Delta\tau_{2135})$	$\tau(SMnSP)$
B Species	
$S_{18} = (1/2^{1/2})(\Delta r_{46} - \Delta r_{56})$	$\nu(P\cdots N)$
$S_{19} = (1/2^{1/2})(\Delta r_{47} - \Delta r_{59})$	$\nu(P-Ph)$
$S_{20} = (1/2^{1/2})(\Delta r_{48} - \Delta r_{5,10})$	$\nu(P-Ph)$
$S_{21} = (1/2^{1/2})(\Delta r_{24} - \Delta r_{35})$	$\nu(P\cdots S)$
$S_{22} = (1/2^{1/2})(\Delta r_{12} - \Delta r_{13})$	$\nu(Mn-S)$
$S_{23} = (1/2)(\Delta\alpha_{67} + \Delta\alpha_{68} - \Delta\alpha_{69} - \Delta\alpha_{6,10})$	$\delta(NPPH)$
$S_{24} = (1/2)(\Delta\alpha_{67} - \Delta\alpha_{68} - \Delta\alpha_{69} + \Delta\alpha_{6,10})$	$\delta(NPPH)$
$S_{25} = (1/2)(\Delta\alpha_{27} + \Delta\alpha_{28} - \Delta\alpha_{39} - \Delta\alpha_{3,10})$	$\delta(SPPH)$
$S_{26} = (1/2)(\Delta\alpha_{27} - \Delta\alpha_{28} - \Delta\alpha_{39} + \Delta\alpha_{3,10})$	$\delta(SPPH)$
$S_{27} = (1/2^{1/2})(\Delta\alpha_{78} - \Delta\alpha_{9,10})$	$\delta(PhPPH)$
$S_{28} = (1/2^{1/2})(\Delta\alpha_{26} - \Delta\alpha_{36})$	$\delta(SPN)$
$S_{29} = (1/2^{1/2})(\Delta\alpha_{14} - \Delta\alpha_{15})$	$\delta(MnSP)$
$S_{30} = (1/2^{1/2})(\Delta\tau_{1246} - \Delta\tau_{1356})$	$\tau(MnSPN)$
$S_{31} = (1/2^{1/2})(\Delta\tau_{2465} - \Delta\tau_{3564})$	$\tau(SPNP)$
$S_{32} = (1/2^{1/2})(\Delta\tau_{3124} - \Delta\tau_{2135})$	$\tau(SMnSP)$

Table V. Bending Stretching ( $K$ ), Angle Bending ( $H$ ), and Repulsive ( $F$ ) Force Constants (mdyn/Å)

	$Co^{II}L'_2$		$Mn^{II}L'_2$		
	R = methyl	R = phenyl	R = methyl	R = phenyl	
$K(M-S)$	0.80	0.45	$K(P-N)$	5.30	5.00
$K(P-S)$	2.20	3.70	$K(P-R)$	2.60	4.80
$H(SPN)$	0.15	0.20	$H(RPR)$	0.13	0.08
$H(PNP)$	0.40	0.40	$H(SMS)$	0.05	0.05
$H(SPR)$	0.14	0.10	$H(MSP)$	0.05	0.05
$H(NPR)$	0.16	0.12			
$F(S\cdots N)$	0.30	0.30	$F(R\cdots R)$	0.30	0.50
$F(P\cdots P)$	0.35	0.35	$F(S\cdots S)$	0.05	0.05
$F(S\cdots R)$	0.18	0.45	$F(M\cdots P)$	0.08	0.05
$F(N\cdots R)$	0.13	0.45			

force field force constants ( $K$ , bond stretching;  $H$ , angle bending;  $F$ , nonadjacent repulsive) for the present stage of refinement are shown in Table V. Also, calculated and observed frequencies and predominant mode assignments from a potential energy distribution calculation are shown in Table VI.

The same procedure was carried out for a 1:1 metal-ligand model of  $Co^{II}L'_2$ , taking average geometric parameters (Table I) determined by X-ray analysis<sup>2</sup> for  $Fe^{II}L'_2$  and  $Ni^{II}L'_2$ . Electronic absorption spectra<sup>1a</sup> of both  $Co^{II}L'_2$  and  $Co^{II}L'_2$  indicated a tetrahedral  $CoS_4$  core structure. The methyl groups of  $L'$  were assumed to exist as a single mass to simplify calculations. The results of this calculation are displayed in Tables V and VI.

**2.  $Cu_4S_6$  Cluster.** A second normal-mode calculation was performed for the  $Cu_4S_6$  core structure that was found by X-ray analysis<sup>8</sup> in  $Cu_4L_3^+$  clusters. A model possessing ex-

(12) (a) Siiman, O.; Fresco, J. *Inorg. Chem.* **1969**, *8*, 1846. (b) Nakamoto, K. "Infrared Spectra of Inorganic and Coordination Compounds", 2nd ed.; Wiley-Interscience: New York, 1969. (c) Siiman, O.; Titus, D. D.; Cowman, C. D.; Fresco, J.; Gray, H. B. *J. Am. Chem. Soc.* **1974**, *96*, 2353.

Table VI. Calculated and Observed Frequencies ( $\text{cm}^{-1}$ ) and Predominant Mode Assignments

$\text{Co}^{\text{II}}\text{L}'_2$				$\text{Mn}^{\text{II}}\text{L}_2$			
calcd	obsd		predominant mode(s)	calcd	obsd		predominant mode(s)
	IR	R			IR	R	
A Species							
876	...	...	$S_1(64) + S_{11}(17)^a$	873	...	...	$S_1(49) + S_{11}(18) + S_4(14)$
731	749 m	749 m	$S_2(82)$	723	715 m	718 vw	$S_2(62) + S_1(17)$
703	713 m	718 w	$S_3(85)$	706	692 sh	690 w, sh	$S_3(54) + S_4(30)$
506	...	511 vs	$S_4(82)$	579	585 mw	580 s	$S_4(42) + S_3(24) + S_{11}(16)$
441	410 m	410 m	$S_{11}(25) + S_{12}(20)$	335	400 m	418 m	$S_8(15) + S_{12}(14)$
305	...	306 ms	$S_5(39) + S_9(27)$	246	...	245 s	$S_5(40) + S_9(39)$
271	...	286 mw	$S_{10}(33) + S_8(28) + S_9(22)$	193	...	200 s	$S_8(38) + S_{10}(25)$
232	...	234 mw	$S_5(33) + S_7(18)$	182	...	187 w	$S_7(21) + S_{12}(19)$
207	...	198 mw	$S_6(41) + S_{10}(15) + S_7(15)$	131	...	128 mw	$S_{14}(32) + S_{13}(19)$
183	...	181 mw	$S_7(33) + S_5(22) + S_9(21)$	105	...	...	$S_6(42) + S_{10}(40)$
138	...	...	$S_{14}(34) + S_{13}(34)$	96	...	...	$S_7(61)$
74	...	...	$S_{15}(23) + S_9(18) + S_{13}(17)$	45	...	...	$S_9(26) + S_{15}(20) + S_{13}(18)$
B Species							
1196	1198 vs	1198 vw	$S_{18}(97)$	1212	1218 vs	...	$S_{18}(96)$
	1187 vs	1187 vw					
747	765 vw	765 vw	$S_{20}(51) + S_{19}(26)$	771	741 m	...	$S_{20}(40) + S_{31}(18)$
689	674 vs	684 m	$S_{19}(63) + S_{20}(23)$	712	700 vs	705 mw	$S_{21}(55) + S_{19}(34)$
545	518 mw	524 mw	$S_{21}(31) + S_{20}(18) + S_{31}(22)$	546	568 s	567 w, sh	$S_{21}(45) + S_{19}(26)$
507	505 ms	...	$S_{21}(54)$	511	518 s	522 w	$S_{20}(49) + S_{31}(24)$
318	318 m	~331 w	$S_{22}(43)$	277	275 m	275 w	$S_{24}(43) + S_{23}(26) + S_{22}(14)$
					285 w, sh	285 w	
303	...	...	$S_{27}(55)$	256	...	...	$S_{22}(37) + S_{26}(29)$
287	...	...	$S_{25}(37) + S_{27}(19)$	190	...	...	$S_{28}(28) + S_{29}(25)$
217	...	...	$S_{26}(37) + S_{22}(22) + S_{24}(16)$	167	...	...	$S_{27}(38)$
186	...	...	$S_{28}(36)$	131	...	...	$S_{22}(39) + S_{21}(23)$
132	...	...	$S_{32}(53)$	87	...	...	$S_{32}(27)$
85	...	...	$S_{24}(36) + S_{31}(24)$	52	...	...	$S_{24}(49) + S_{31}(30)$

<sup>a</sup> Percent contribution in parentheses.

actly  $T_d$  point symmetry, shown in Figure 3, was adopted. The adamantane-like cage structure in  $\text{Cu}_4\text{L}_3^+$  very closely approaches the idealized structure, with sulfur atoms at the corners of an octahedron and Cu atoms at the centers of alternate octahedral faces. Bond distances and angles in the model were  $r(\text{Cu-S}) = 2.263 \text{ \AA}$ ,  $\alpha(\text{CuSCu}) = 70.6^\circ$ ,  $\alpha(\text{SCuS}) = 120^\circ$ . An average S...S edge distance of  $3.920 \text{ \AA}$  was transferred from the  $\text{Cu}_4\text{L}_3^+$  structure. The 24 genuine normal vibrations ( $2 A_1 + 2 E + 2 T_1 + 4 T_2$ ) were analyzed. The 10-atom model gave 30 internal (12 Cu-S bond stretching, 12 SCuS angle bending, and 6 CuSCu angle bending) coordinates which were divided into the  $3 A_1$ ,  $3 E$ ,  $2 T_1$ , and  $5 T_2$  symmetry coordinates listed in Table VII. Symmetry coordinates were constructed in the usual way<sup>13</sup> such that the E species transformed as the components of the two-dimensional matrix for  $(2z^2 - x^2 - y^2, x^2 - y^2)$ ,  $T_1$  species transformed as the components of the three-dimensional matrices for the rotations ( $R_x, R_y, R_z$ ), and  $T_2$  species transformed as the components of the three-dimensional matrices for the translations ( $x, y, z$ ) under all symmetry operations of the  $T_d$  point group. In the T species care was taken to group degenerate species, unstarred, starred, and double-starred, according to whether they transformed like the twofold rotations  $C_2(x)$ ,  $C_2(y)$ , or  $C_2(z)$ , respectively. This<sup>13,14</sup> prevents the occurrence of cross terms when the G and F matrices are blocked by the symmetry coordinate transformation. Redundancies,  $1 A_1 + 1 E + 1 T_2$ , gave zero eigenvalues in the G and GF matrices. Force constants and calculated-observed frequencies are shown in Table VIII.

**C. PNP Bonding.** The noticeable absence of an infrared or Raman band assignable to  $\nu_s(\text{P}\cdots\text{N}\cdots\text{P})$  in dithioimidodiphosphinates was somewhat surprising. In any case the most

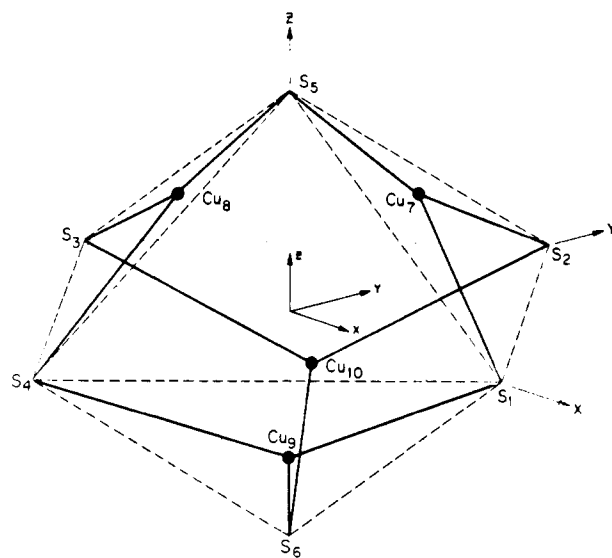


Figure 3. Structural model for the  $\text{Cu}_4\text{S}_6$  core of copper cluster compounds.

intense resonance Raman band in  $\text{Cu}^{\text{II}}\text{L}_2$  was identified as  $\nu_s(\text{P}\cdots\text{N}\cdots\text{P})$  at  $813 \text{ cm}^{-1}$ . Normal-mode calculations further support this assignment. When the calculated  $\nu_{\text{as}}(\text{PNP})$  frequency is fitted to an observed band at  $1220 \text{ cm}^{-1}$ ,  $\nu_s(\text{PNP})$  is calculated to appear in the  $750\text{--}850\text{-cm}^{-1}$  region. Also, RR band intensities<sup>15</sup> depend on the nature of the electronic excited state that is involved, and, therefore, large bond polarizability derivatives are not the only source of intensity. Rather, Franck-Condon overlaps<sup>16</sup> that depend on  $\Delta K$  (force constant)

(13) Wilson, E. B., Jr.; Decius, J. C.; Cross, P. C. "Molecular Vibrations"; McGraw-Hill: New York, 1955.

(14) Siiman, O.; Fresco, J. *Spectrochim. Acta, Part A* 1971, 27A, 673.

(15) (a) Siebrand, W.; Zgierski, M. Z. *Excited States* 1979, 4, 1. (b) Clark, R. J. H.; Stewart, B. *Struct. Bonding (Berlin)* 1979, 36, 1.

Table VII. Symmetry Coordinates for Cu<sub>4</sub>S<sub>6</sub> Core Model in T<sub>d</sub> Symmetry

coordinate	mode
A <sub>1</sub> Species	
$S_1 = (1/2(3^{1/2}))(\Delta r_{71} + \Delta r_{91} + \Delta r_{10,3} + \Delta r_{83} + \Delta r_{72} + \Delta r_{84} + \Delta r_{10,2} + \Delta r_{75} + \Delta r_{10,6} + \Delta r_{85} + \Delta r_{96})$	$\nu(\text{Cu-S})$
$S_2 = (1/2(3^{1/2}))(\Delta\alpha_{1,7,2} + \Delta\alpha_{4,9,1} + \Delta\alpha_{2,10,3} + \Delta\alpha_{3,8,4} + \Delta\alpha_{2,7,5} + \Delta\alpha_{4,8,5} + \Delta\alpha_{4,9,6} + \Delta\alpha_{2,10,6} + \Delta\alpha_{1,7,5} + \Delta\alpha_{3,10,6} + \Delta\alpha_{3,8,5} + \Delta\alpha_{1,9,6})$	$\delta(\text{SCuS})$
$S_3 = (1/6^{1/2})(\Delta\alpha_{7,5,8} + \Delta\alpha_{10,6,9} + \Delta\alpha_{9,1,7} + \Delta\alpha_{10,3,8} + \Delta\alpha_{7,2,10} + \Delta\alpha_{8,4,9})$	$\delta(\text{CuSCu})$
E Species	
$S_4 = (1/2(6^{1/2}))(2\Delta r_{75} + 2\Delta r_{10,6} + 2\Delta r_{85} + 2\Delta r_{96} - \Delta r_{71} - \Delta r_{91} - \Delta r_{10,3} - \Delta r_{83} - \Delta r_{72} - \Delta r_{84} - \Delta r_{94} - \Delta r_{10,2})$	$\nu(\text{Cu-S})$
$S_5 = (1/2(6^{1/2}))(2\Delta\alpha_{1,7,2} + 2\Delta\alpha_{4,9,1} + 2\Delta\alpha_{2,10,3} + 2\Delta\alpha_{3,8,4} - \Delta\alpha_{2,7,5} - \Delta\alpha_{4,8,5} - \Delta\alpha_{4,9,6} - \Delta\alpha_{2,10,6} - \Delta\alpha_{1,7,5} - \Delta\alpha_{3,10,6} - \Delta\alpha_{3,8,5} - \Delta\alpha_{1,9,6})$	$\delta(\text{SCuS})$
$S_6 = (1/2(3^{1/2}))(2\Delta\alpha_{7,5,8} + 2\Delta\alpha_{10,6,9} - \Delta\alpha_{9,1,7} - \Delta\alpha_{10,3,8} - \Delta r_{7,2,10} - \Delta\alpha_{8,4,9})$	$\delta(\text{CuSCu})$
$S_4^* = (1/2(2^{1/2}))(\Delta r_{71} + \Delta r_{91} + \Delta r_{10,3} + \Delta r_{83} - \Delta r_{72} - \Delta r_{84} - \Delta r_{94} - \Delta r_{10,2})$	$\nu(\text{Cu-S})$
$S_5^* = (1/2(2^{1/2}))(\Delta\alpha_{2,7,5} + \Delta\alpha_{4,8,5} + \Delta\alpha_{4,9,6} + \Delta\alpha_{2,10,6} - \Delta\alpha_{1,7,5} - \Delta\alpha_{3,10,6} - \Delta\alpha_{3,8,5} - \Delta\alpha_{1,9,6})$	$\delta(\text{SCuS})$
$S_6^* = (1/2)(\Delta\alpha_{9,1,7} + \Delta\alpha_{10,3,8} - \Delta\alpha_{7,2,10} - \Delta\alpha_{8,4,9})$	$\delta(\text{CuSCu})$
T <sub>1</sub> Species	
$S_7 = (1/2(2^{1/2}))(\Delta r_{72} - \Delta r_{84} + \Delta r_{94} - \Delta r_{10,2} - \Delta r_{75} + \Delta r_{10,6} + \Delta r_{85} - \Delta r_{96})$	$\nu(\text{Cu-S})$
$S_8 = (1/2(2^{1/2}))(\Delta\alpha_{1,7,2} + \Delta\alpha_{4,9,1} - \Delta\alpha_{2,10,3} - \Delta\alpha_{3,8,4} - \Delta\alpha_{1,7,5} + \Delta\alpha_{3,10,6} + \Delta\alpha_{3,8,5} - \Delta\alpha_{1,9,6})$	$\delta(\text{SCuS})$
$S_7^* = (1/2(2^{1/2}))(\Delta r_{71} - \Delta r_{91} + \Delta r_{10,3} - \Delta r_{83} - \Delta r_{75} - \Delta r_{10,6} + \Delta r_{85} + \Delta r_{96})$	$\nu(\text{Cu-S})$
$S_8^* = (1/2(2^{1/2}))(\Delta\alpha_{1,7,2} - \Delta\alpha_{4,9,1} + \Delta\alpha_{2,10,3} - \Delta\alpha_{3,8,4} - \Delta\alpha_{2,7,5} + \Delta\alpha_{4,8,5} + \Delta\alpha_{4,9,6} - \Delta\alpha_{2,10,6})$	$\delta(\text{SCuS})$
$S_7^{**} = (1/2(2^{1/2}))(\Delta r_{71} - \Delta r_{91} - \Delta r_{10,3} + \Delta r_{83} - \Delta r_{72} - \Delta r_{84} + \Delta r_{94} + \Delta r_{10,2})$	$\nu(\text{Cu-S})$
$S_8^{**} = (1/2(2^{1/2}))(\Delta\alpha_{2,7,5} + \Delta\alpha_{4,8,5} - \Delta\alpha_{4,9,6} - \Delta\alpha_{2,10,6} - \Delta\alpha_{1,7,5} + \Delta\alpha_{3,10,6} - \Delta\alpha_{3,8,5} + \Delta\alpha_{1,9,6})$	$\delta(\text{SCuS})$
T <sub>2</sub> Species	
$S_9 = (1/2)(\Delta r_{71} + \Delta r_{91} - \Delta r_{10,3} - \Delta r_{83})$	$\nu(\text{Cu-S})$
$S_{10} = (1/2(2^{1/2}))(\Delta r_{72} - \Delta r_{84} + \Delta r_{94} - \Delta r_{10,2} + \Delta r_{75} - \Delta r_{10,6} - \Delta r_{85} + \Delta r_{96})$	$\nu(\text{Cu-S})$
$S_{11} = (1/2(2^{1/2}))(\Delta\alpha_{2,7,5} - \Delta\alpha_{4,8,5} + \Delta\alpha_{4,9,6} - \Delta\alpha_{2,10,6})$	$\delta(\text{SCuS})$
$S_{12} = (1/2(2^{1/2}))(\Delta\alpha_{1,7,2} + \Delta\alpha_{4,9,1} - \Delta\alpha_{2,10,3} - \Delta\alpha_{3,8,4} + \Delta\alpha_{1,7,5} - \Delta\alpha_{3,10,6} - \Delta\alpha_{3,8,5} + \Delta\alpha_{1,9,6})$	$\delta(\text{CuS})$
$S_{13} = (1/2(2^{1/2}))(\Delta\alpha_{9,1,7} - \Delta\alpha_{10,3,8})$	$\delta(\text{CuSCu})$
$S_9^* = (1/2)(\Delta r_{72} - \Delta r_{84} - \Delta r_{94} + \Delta r_{10,2})$	$\nu(\text{Cu-S})$
$S_{10}^* = (1/2(2^{1/2}))(\Delta r_{71} - \Delta r_{91} + \Delta r_{10,3} - \Delta r_{83} + \Delta r_{75} + \Delta r_{10,6} - \Delta r_{85} - \Delta r_{96})$	$\nu(\text{Cu-S})$
$S_{11}^* = (1/2)(\Delta\alpha_{1,7,5} + \Delta\alpha_{3,10,6} - \Delta\alpha_{3,8,5} - \Delta\alpha_{1,9,6})$	$\delta(\text{SCuS})$
$S_{12}^* = (1/2(2^{1/2}))(\Delta\alpha_{1,7,2} - \Delta\alpha_{4,9,1} + \Delta\alpha_{2,10,3} - \Delta\alpha_{3,8,4} + \Delta\alpha_{2,7,5} - \Delta\alpha_{4,8,5} - \Delta\alpha_{4,9,6} + \Delta\alpha_{2,10,6})$	$\delta(\text{CuS})$
$S_{13}^* = (1/2(2^{1/2}))(\Delta\alpha_{7,2,10} - \Delta\alpha_{8,4,9})$	$\delta(\text{CuSCu})$
$S_9^{**} = (1/2)(\Delta r_{75} - \Delta r_{10,6} + \Delta r_{85} - \Delta r_{96})$	$\nu(\text{Cu-S})$
$S_{10}^{**} = (1/2(2^{1/2}))(\Delta r_{71} - \Delta r_{91} - \Delta r_{10,3} + \Delta r_{83} + \Delta r_{72} + \Delta r_{84} - \Delta r_{94} - \Delta r_{10,2})$	$\nu(\text{Cu-S})$
$S_{11}^{**} = (1/2)(\Delta\alpha_{1,7,2} - \Delta\alpha_{4,9,1} - \Delta\alpha_{2,10,3} + \Delta\alpha_{3,8,4})$	$\delta(\text{CuS})$
$S_{12}^{**} = (1/2(2^{1/2}))(\Delta\alpha_{2,7,5} + \Delta\alpha_{4,8,5} - \Delta\alpha_{4,9,6} - \Delta\alpha_{2,10,6} + \Delta\alpha_{1,7,5} - \Delta\alpha_{3,10,6} + \Delta\alpha_{3,8,5} - \Delta\alpha_{1,9,6})$	$\delta(\text{CuS})$
$S_{13}^{**} = (1/2(2^{1/2}))(\Delta\alpha_{7,5,8} - \Delta\alpha_{10,6,9})$	$\delta(\text{CuSCu})$

Table VIII. Calculated and Observed Frequencies (cm<sup>-1</sup>) and Predominant Mode Assignments for Cu<sub>4</sub>S<sub>6</sub> Core<sup>a</sup>

calcd	Cu <sub>4</sub> L <sub>3</sub> <sup>+</sup>		predominant mode
	IR	R	
A <sub>1</sub> Species			
272	275	272	$\nu(\text{Cu-S})$
171		175	$\delta(\text{CuSCu})$
E Species			
267	...	255	$\nu(\text{Cu-S})$
127			$\delta(\text{SCuS})$
T <sub>1</sub> Species			
219	...	...	$\nu(\text{Cu-S})$
145	...	...	$\delta(\text{SCuS})$
T <sub>2</sub> Species			
271	275	277	$\nu(\text{Cu-S})$
244	242	245	$\delta(\text{SCuS})$
186		175	$\nu(\text{Cu-S})$
110			$\delta(\text{CuS})$

<sup>a</sup>  $K(\text{Cu-S}) = 0.50$  mdyn/Å;  $H(\text{SCuS}) = 0.10$ ,  $F(\text{S} \cdots \text{S}) = 0.15$  mdyn/Å;  $H(\text{CuSCu}) = 0.05$ ,  $F(\text{Cu} \cdots \text{Cu}) = 0.20$  mdyn/Å.

and  $\Delta r$  (bond distance) between ground and excited states are important in determining band intensities. In the quantum-mechanical view of Raman scattering the classical polarizability derivative is replaced by  $(\alpha_{\rho\sigma})_{m,n}$ , where  $m$  and  $n$  are

the initial and final states, and is represented by the Kramers-Heisenberg dispersion equation<sup>15</sup>

$$(\alpha_{\rho\sigma})_{m,n} = \sum_e \left[ \frac{\langle m|M_\rho|e\rangle \langle e|M_\sigma|n\rangle}{E_e - E_m - E_0} + \frac{\langle m|M_\sigma|e\rangle \langle e|M_\rho|n\rangle}{E_e - E_n + E_0} \right]$$

The sum is taken over excited electronic states,  $e$ , of the molecule. When  $\nu_0 \rightarrow (\nu_e - \nu_m)$ , a few terms dominate because of small denominators. If the Born-Oppenheimer approximation is applied

$$|e\rangle = \psi_e(q, Q)\phi_e(Q)$$

and  $\psi_e$  is expanded in a Taylor series

$$\psi_e(q, Q) = \psi_e(q, Q=0) + \left( \frac{\partial \psi_e}{\partial Q} \right)_{Q=0} Q + \dots$$

then, for totally symmetric vibrations,<sup>17</sup> the first term in the series for  $(\alpha_{\rho\sigma})_{m,n}$  is nonzero. For a single excited state

$$(\alpha_{\rho\sigma})_{0,1} = |\langle g|M_\rho|e\rangle_0|^2 \sum_v \frac{\langle 0|v\rangle \langle v|1\rangle}{E_e - E_g - E_0}$$

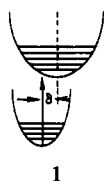
In the Condon approximation that is implied the value of  $M_\rho$  is that at  $Q = 0$  and  $M_\sigma$  is not a function of the vibrational transition that accompanies the electronic transition.

(16) (a) Ruamps, J. C. R. *Hebdomadae Acad. Sci.* **1956**, *243*, 2034. (b) Sushchinskii, M. M. "Raman Spectra of Molecules and Crystals"; Keter: New York, 1972.

(17) Tang, J.; Albrecht, A. C. In "Raman Spectroscopy, Theory and Practice"; Szymanski, H. A., Ed.; Plenum Press: New York, 1967; Vol. 1, p 168.

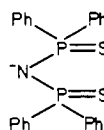
Therefore, for  $A_{1(g)}$  vibrations, resonance Raman intensity is large (1) when  $I$  absorption is large (given by value of transition moment  $\langle g|M_{\sigma}|e\rangle$ ), (2) when some products of Franck-Condon overlaps,  $\langle 0|v\rangle\langle v|1\rangle$ , are large, and (3) when  $\nu_0 \rightarrow \nu$  (electronic absorption band).

Franck-Condon overlaps<sup>16</sup> (shown pictorially by 1) are large

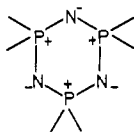


when  $\delta$  and/or  $\Delta K$  ( $K = (\partial^2 V / \partial Q^2)_{Q=0}$ ) are large. In  $\text{Cu}^{\text{II}}\text{L}_2$ , relatively large intensification of  $\nu_s(\text{PNP})$  at  $813\text{ cm}^{-1}$  and  $\delta_s(\text{PNP})$  at  $425\text{ cm}^{-1}$ , compared to  $\nu(\text{P}^{\leftarrow}\text{S})$  at  $580\text{ cm}^{-1}$  and  $\nu(\text{Cu}-\text{S})$  at  $290$  and  $210\text{ cm}^{-1}$  suggests that Franck-Condon factors favor activation of PNP vibrations over others. Although a  $\sigma(\text{S}) \rightarrow d_{\sigma}(\text{Cu})$  transition assignment for the 585-nm absorption band is favored, the relatively low RR enhancement of  $\nu(\text{Cu}-\text{S})$  suggests that those orbitals,  $\sigma(\text{S})$  and  $d_{\sigma}(\text{Cu})$  directed along the Cu-S bond, cannot be the major contributors to MO levels in the resonant electronic transition. In a  $\pi(\text{L}) \rightarrow d_{\sigma}(\text{Cu})$  transition the symmetry of the two MO levels does not match; thus, we expect little overlap and a low transition moment. A reasonable assignment which takes into account the intensity of the absorption band as well as the RR data is  $d_{\pi}(\text{Cu}) \rightarrow \pi^*(\text{L})$ . Franck-Condon factors favor activation of PNP vibrations if the  $\pi^*(\text{L})$  contains a major contribution from N- and P-localized  $\pi$  orbitals.

Bent triatomics ( $C_{2v}$  point symmetry) of the type  $\text{XY}_2$ , in particular,<sup>18</sup>  $\text{Cl}_2\text{O}$ , show all three fundamentals in both infrared and Raman spectra. The symmetric  $\nu_1(\text{Y}-\text{X}-\text{Y})$  stretching band appears as the most intense Raman band. Phosphazenes<sup>9</sup> that are cyclic trimers or tetramers of  $\text{R}_2\text{PN}$  also show an intense symmetric  $\text{P}_3\text{N}_3$  ring stretching Raman band in the  $750\text{--}800\text{ cm}^{-1}$  region. Bonding<sup>19</sup> within cyclophosphazene rings has been analyzed in detail. Both in-plane and out-of-plane  $p_{\pi}(\text{N})\text{--}d_{\pi}(\text{P})$  bondings have been proposed in addition to the  $\sigma$ -bonded  $\text{P}_3\text{N}_3$  skeleton. Bonding about nitrogen in imidodiphosphinates, however, differs somewhat from that at nitrogen in cyclophosphazenes. In the  $\text{L}^-$  ligand the nitrogen atom is formally negatively charged as

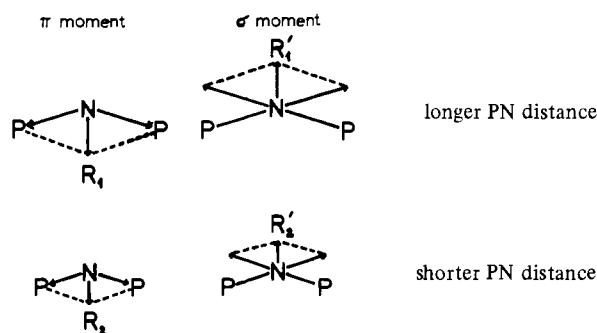


and this negative electron density is delocalized when binding through S atoms takes place to an electropositive metal ion. In  $[\text{R}_2\text{NP}]_3$  the fifth valence electron of P is assumed to occupy a d orbital while the N atom has a one-electron  $p_{\pi}$  (out-of-plane) orbital and a doubly occupied in-plane lone pair. Only in the improbable ionic limit



does nitrogen carry a negative charge. We, therefore, anticipate that the degree of  $\text{N} \rightarrow \text{P}$ ,  $p_{\pi} \rightarrow d_{\pi}$  back-bonding in

Chart I



imidodiphosphinates is much greater than in cyclophosphazenes. Substituent (methyl for phenyl, oxygen for sulfur, interchange of metal ion) and geometry (nonplanar vs. planar chelate ring, change in P-N-P angle) changes have no noticeable effect on the lack of intensity in  $\nu_s(\text{PNP})$ . In compounds that contain the isoelectronic unit  $\text{P}-\text{O}-\text{P}$  a symmetric  $\nu_s(\text{POP})$  band has been identified<sup>20</sup> as a polarized Raman band near  $611\text{ cm}^{-1}$ . No substantial  $p_{\pi}(\text{O})\text{--}d_{\pi}(\text{P})$  back-bonding can, however, be associated with the much lower  $\nu_{as}(\text{POP})$  and  $\nu_s(\text{POP})$  frequencies. These are similar to  $\nu_{as}(\text{P-N-P})$  and  $\nu_s(\text{P-N-P})$  frequencies of the N-protonated ligands. An explanation for the absence of IR and R intensity in  $\nu_s(\text{PNP})$  is offered in terms of the special bonding effects in the  $\text{P-N-P}$  moiety.

$\sigma(\text{P} \rightarrow \text{N}, \chi_{\text{N}} > \chi_{\text{P}})$  and  $\pi(\text{N} \rightarrow \text{P})$  back-bonding effects with regard to bond moments and polarizabilities are directly opposed to each other in the PNP group. Therefore, at extremes of the symmetric PNP bond stretching mode displacement we envision the situation shown in Chart I. If  $\sigma(\text{P} \rightarrow \text{N})$  and  $\pi(\text{N} \rightarrow \text{P})$  bonding effects have the same magnitude, then exact cancellation of resultant bond moments  $R_1$  and  $R_1'$  or  $R_2$  and  $R_2'$  can occur at the same bond stretching displacement values such that no change in the total moment takes place during the vibration. Similar arguments apply to bond polarizability changes. The result is very low  $\partial\mu/\partial R$  and  $\partial\alpha/\partial R$  values and thus very little or no infrared or Raman intensity in this fundamental.

During the PNP bending vibration no change in PN  $\sigma$  overlap or out-of-plane  $\pi$  overlap is expected if the PN bond distance does not change. However, the in-plane  $\pi$  overlap between the nitrogen lone pair and the in-plane  $d_{\pi}$  of the phosphorus atoms does change as the PNP angle changes during the bending mode. This contribution offsets the total balance of  $\pi$ - and  $\sigma$ -bond moment and polarizability changes and produces a net change in dipole moment and polarizability. Thus,  $\delta(\text{PNP})$  was observed in both infrared and Raman spectra near  $420\text{ cm}^{-1}$ .

Though the same back-bonding arguments can be invoked for the  $\text{P}^{\leftarrow}\text{S}$  stretching mode, the extent of multiple bonding in the PS bond is much less. In addition, sulfur and phosphorus electronegativities are much closer in value and thus lead to a much less polar bond.

**D. Metal-Ligand Bonding.** Bond stretching force constants,  $K(\text{Mn-S}) = 0.45$ ,  $K(\text{Co-S}) = 0.80$ , and  $K(\text{Cu-S}) = 0.50$   $\text{mdyn}/\text{\AA}$ , show that metal-sulfur bonding in the tetraphenyl ligand is substantially weaker than in the tetramethyl ligand. The same trend is reinforced by the values of the force constants,  $K(\text{PS}) = 3.70\text{ mdyn}/\text{\AA}$  in  $\text{Mn}^{\text{II}}\text{L}_2$ , and  $K(\text{PS}) = 2.20\text{ mdyn}/\text{\AA}$  in  $\text{Co}^{\text{II}}\text{L}_2$ . The  $1.50\text{ mdyn}/\text{\AA}$  lower value reflects stronger M-S bonding to the methyl-substituted ligand and a parallel decrease in the PS bond order. Values of PN

(18) Renard, J. J.; Bolker, H. I. *Chem. Rev.* **1976**, *76*, 487.

(19) (a) Allcock, H. R. "Phosphorus-Nitrogen Compounds"; Academic Press: New York, 1972. (b) Krishnamurthy, S. S.; Sau, A. C.; Woods, M. *Adv. Inorg. Chem. Radiochem.* **1978**, *21*, 41.

(20) Emsley, J.; Middleton, T. B.; Williams, J. K. *J. Chem. Soc., Dalton Trans.* **1973**, 2701.

constants, though, show little difference.

Relative to  $K(M-S)$  values that were obtained in normal-coordinate analyses of other metal-sulfur complexes<sup>21</sup> such as dithioacetylacetonates,<sup>12a</sup> monothioacetylacetonates,<sup>12c</sup> and dithienes,<sup>11</sup> results that were obtained herein for dithioimidodiphosphinates represent the lowest  $K(M-S)$  values. Both the tetrahedral geometry (as opposed to square planar)

and the nature of the ligand (not a thiolate sulfur donor) probably contribute to the low metal-ligand bond strengths. Some intensification of Cu(I)-S Raman bands in the 200-300-cm<sup>-1</sup> region for Cu<sup>I</sup>L<sub>3</sub> and Cu<sup>I</sup>L<sub>3</sub><sup>+</sup> clusters in comparison to Raman band intensities in the same region for bis chelates such as Mn<sup>II</sup>L<sub>2</sub> might be surmised to arise from weak Cu...Cu bonding interactions.

Registry No. Mn<sup>II</sup>L<sub>2</sub>, 40362-04-7; Co<sup>II</sup>L<sub>2</sub>, 31747-72-5; Co<sup>II</sup>L<sub>2</sub>, 31747-71-4; Cu<sup>I</sup>L<sub>3</sub><sup>+</sup>, 65404-72-0.

(21) Siiman, O. *Inorg. Chem.* 1980, 19, 2889.

Contribution from the Institute for Molecular Science, Myodaiji, Okazaki 444, Japan, and the Department of Industrial Chemistry, Kumamoto University, Kurokami, Kumamoto 860, Japan

## Bonding in Ni(PH<sub>3</sub>)<sub>2</sub>(C<sub>2</sub>H<sub>4</sub>) and Ni(PH<sub>3</sub>)<sub>2</sub>(C<sub>2</sub>H<sub>2</sub>). An ab Initio SCF-MO Study

KAZUO KITaura,<sup>1a</sup> SHIGEYOSHI SAKAKI,<sup>1b</sup> and KEIJI MOROKUMA\*<sup>1a</sup>

Received March 12, 1980

Ab initio MO calculations were carried out on Ni(PH<sub>3</sub>)<sub>2</sub>(C<sub>2</sub>H<sub>4</sub>) and Ni(PH<sub>3</sub>)<sub>2</sub>(C<sub>2</sub>H<sub>2</sub>). C-C bond lengths and bending angles of complexed ethylene and acetylene were determined. The binding energy was found to be larger in the acetylene complex than in the ethylene complex. The relative magnitude of  $\sigma$  donation and  $\pi$  back-donation was revealed through an analysis of binding energy and electron distribution. The influence of other ligands on the Ni-C<sub>2</sub>H<sub>4</sub> bonding was discussed by comparing PH<sub>3</sub> with NH<sub>3</sub> as ligands.

### Introduction

The Dewar-Chart-Duncanson bonding model<sup>2</sup> has been the basis for qualitative understanding of chemical and physical properties of metal-olefin complexes. A number of semi-empirical and ab initio MO calculations have been performed for a more quantitative description of the bonding.<sup>3</sup> However, most of these prior studies have discussed the relative importance of  $\sigma$  donation and  $\pi$  back-donation solely on the basis of the electron population on the metal atom and olefin. In the present work, we will attempt to reveal how  $\sigma$  donation and  $\pi$  back-donation contribute to the metal-olefin bond, through an analysis of the binding energy, as well as the electron distribution. We apply the scheme of energy decomposition analysis (EDA),<sup>4</sup> developed for studying intermolecular interactions. EDA enables us to understand the origin of bonding in terms of various meaningful interactions: electrostatic (Coulombic), exchange-repulsion, polarization, charge-transfer, and others. Though EDA and similar methods<sup>5</sup> have been widely applied to various types of intermolecular complexes,<sup>4a</sup> only a few applications have been made for transition-metal complexes.<sup>6</sup> Sakaki et al. have recently

studied the bonding nature and stereochemistry of metal-carbon dioxide complexes by EDA with the ab initio SCF-MO method.<sup>7</sup> Ziegler and Rauk have carried out a similar analysis with a Hartree-Fock-Slater method for transition-metal ethylene and carbonyl complexes.<sup>8</sup>

In this paper, after giving the definition of energy components relevant to the  $\sigma$  donation and  $\pi$  back-donation, we will study the nature of bonding between Ni(PH<sub>3</sub>)<sub>2</sub> and C<sub>2</sub>H<sub>4</sub> in detail. The influence of other ligands on the Ni-C<sub>2</sub>H<sub>4</sub> bonding will also be discussed. A comparison will be made between Ni-C<sub>2</sub>H<sub>4</sub> and -C<sub>2</sub>H<sub>2</sub> bonding.

### Computational Procedures

We have assumed that the complexes Ni(PH<sub>3</sub>)<sub>2</sub>(C<sub>2</sub>H<sub>4</sub>), Ni(PH<sub>3</sub>)<sub>2</sub>(C<sub>2</sub>H<sub>2</sub>), and Ni(NH<sub>3</sub>)<sub>2</sub>(C<sub>2</sub>H<sub>4</sub>) are singlets in their ground states, as was also assumed in previous studies.<sup>21</sup> As will be discussed later, with the stabilizing PH<sub>3</sub> ligands the electron configuration of these complexes is close to d<sup>10</sup>, which would favor a singlet state. All calculations were performed with use of the closed-shell restricted Hartree-Fock (RHF) method.

**Basis Set and Geometry.** Ab initio SCF-MO calculations were carried out with use of the IMSPACK program system.<sup>9</sup> The basis sets used were the 4-31G set<sup>10a</sup> for ligand atoms and the [4s3p2d] contracted set for nickel atoms. The [4s3p2d] set was contracted from the (11s7p5d) primitive Gaussian set, which was modified from (12s6p4d)<sup>10b</sup> by deleting the two most diffuse s-type functions and adding an s-type, a p-type, and a d-type function with the exponents 0.2, 0.25, and 0.2, respectively. The 3s-type functions arising from the totally symmetric linear combination of d-type functions were removed from the basis set. The basis set used here was found to give reasonable binding energies and geometries.<sup>11</sup>

- (1) (a) Institute for Molecular Science. (b) Kumamoto University.
- (2) Dewar, M. J. S. *Bull. Soc. Chim. Fr.* 1951, 79. Chart, J.; Duncanson, L. A. *J. Chem. Soc.* 1953, 2939.
- (3) Semiempirical calculations, for example, are given in: Tatsumi, K.; Fueno, T.; Nakamura, A.; Otuska, S. *Bull. Chem. Soc. Jpn.* 1976, 49, 2170. Sakaki, S.; Kato, H.; Kawamura, T. 1975, 48, 195. Wheelock, K. S.; Nelson, J. H.; Cusachs, L. C.; Jonassen, H. B. *J. Am. Chem. Soc.* 1970, 92, 5110. Nelson, J. H.; Wheelock, K. S.; Cusachs, L. C.; Jonassen, H. B. *Inorg. Chem.* 1972, 11, 422. Rösch, N.; Messmer, R. P.; Johnson, K. H. *J. Am. Chem. Soc.* 1974, 96, 3855. Ab initio calculations are given in: Basch, H. *J. Chem. Phys.* 1972, 56, 441. Swope, W. C.; Sachafer III, H. F. *Mol. Phys.* 1977, 34, 1037.
- (4) (a) Morokuma, K. *Acc. Chem. Res.* 1977, 10, 294. (b) Kitaura, K.; Morokuma, K. *Int. J. Quantum Chem.* 1976, 10, 325.
- (5) Kollman, P. A.; Allen, L. C. *J. Phys.* 1970, 52, 5085. Dreyfus, M.; Maigret, B.; Pullman, A. *Theor. Chim. Acta* 1970, 17, 109.
- (6) Noell, J. O.; Morokuma, K. *Inorg. Chem.* 1979, 18, 2774. Demoulin, D.; Pullman, A. *Theor. Chim. Acta* 1978, 49, 161.

- (7) Sakaki, S.; Kitaura, K.; Morokuma, K., to be submitted for publication in *Inorg. Chem.*
- (8) Ziegler, T.; Rauk, A. *Inorg. Chem.* 1979, 18, 1558, 1755.
- (9) Morokuma, K.; Kato, S.; Kitaura, K.; Ohmine, I.; Sakai, S.; unpublished data. The ab initio program package consists of GAUSSIAN 70, HONDO, and many of our own routines.
- (10) (a) Ditchfield, R.; Hehre, W. J.; Pople, J. A. *J. Chem. Phys.* 1970, 52, 5001. (b) Roos, B.; Veillard, A.; Vinot, G. *Theor. Chim. Acta* 1971, 20, 1.